Discriminatory Influence of Glu-376→Asp Mutation in Medium-Chain Acyl-CoA Dehydrogenase on the Binding of Selected CoA-Ligands: Spectroscopic, Thermodynamic, Kinetic, and Model Building Studies†

D. K. Srivastava* and Kevin L. Peterson

Biochemistry Department, North Dakota State University, Fargo, North Dakota 58105

Received February 18, 1998; Revised Manuscript Received April 17, 1998

ABSTRACT: We investigated the influence of Glu-376→Asp (E376D) mutation on the UV/visible spectral, thermodynamic, and kinetic properties for the interaction of structurally different types of CoA-ligands (viz., octenoyl-CoA, acetoacetyl-CoA, and indoleacryloyl-CoA) to human liver medium-chain acyl-CoA dehydrogenase (MCAD). Whereas the E376D mutation had minimal/negligible effect on the above properties for the binding of octenoyl-CoA to the enzyme, it had pronounced effects (albeit in opposite directions) for the binding of acetoacetyl-CoA and indoleacryloyl-CoA to the enzyme. In the case of acetoacetyl-CoA, the spectrum of the enzyme−ligand complex (in the charge-transfer region; $\lambda_{max} = 545$ nm) was 1.8-fold more pronounced, and the $\Delta H°$ value for the binding of acetoacetyl-CoA to the enzyme was 5.6 kcal/mol more favorable with wild-type as compared to the E376D mutant enzyme. The kinetic data revealed that the above effects were related to an increase in the dissociation "off-rate" of acetoacetyl-CoA from the enzyme−acetoacetyl-CoA complex. In contrast, in the case of IACoA, the resultant UV/visible spectrum of the enzyme−IACoA complex ($\lambda_{max} = 416$ nm) was 2.7-fold less pronounced, and the $\Delta H°$ value of the enzyme−IACoA complex was 6.4 kcal/mol less favorable with the wild-type than the E376D mutant enzyme. The latter effects were supported by the fact that the above mutation impaired the dissociation "off-rate" of IACoA from the enzyme−IACoA complex by 5.7-fold. Molecular model building studies revealed that the discriminatory influence of the E376D mutation on the spectral, thermodynamic, and kinetic properties of the enzyme−ligand complexes is due to ligand-specific changes in the spatial relationship between the FAD and CoA-ligands at the enzyme site. Arguments are presented that the "void" created by excision of a methylene group from Glu-376 (upon Glu-376→Asp mutation) is adjusted differently upon interaction with structurally different types of CoA-ligands.

The medium-chain acyl-CoA dehydrogenase (MCAD)[1]-catalyzed reaction proceeds via abstraction of the α (*pro-R*) hydrogen from acyl-CoA substrate by the active site base Glu-376, concomitant with the transfer of the *β*-hydrogen in the form of a hydride to the N-5 position of the isoalloxazine ring of the enzyme-bound FAD (eq 1; for reviews, see *1*−*3*).

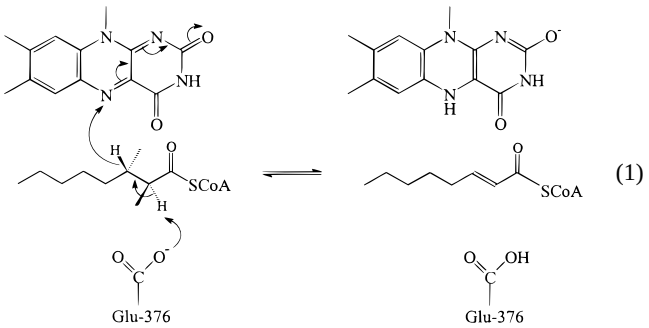

(1)

One of the most interesting aspects of the above reaction is that the reaction product, enoyl-CoA, remains fairly tightly bound to the reduced enzyme (E−$FADH_2$) site, and it is stabilized via formation of the E−$FADH_2$−enoyl-CoA charge-transfer complex (*1*, *2*). The latter complex is further characterized by the polarized form of the carbonyl group of enoyl-CoA within the reduced enzyme site (*4*−*7*). Due to a marked stability of the E−$FADH_2$−enoyl-CoA charge-transfer complex, the reductive half-reaction of the enzyme, involving octanoyl-CoA as a physiological substrate, is essentially confined to a single-turnover condition (*8*, *9*). The repetitive turnover of the enzyme is maintained via transfer of reducing equivalents from the above complex to suitable electron acceptors, such as electron-transferring flavoprotein (ETF) or ferricenium hexafluorophosphate ($FcPF_6$), during the "oxidative half-reaction" of the enzyme (*10*, *11*; eq 2).

† This work was supported by grants from the National Science Foundation (MCB-9507292) and the American Heart Association, National Center (AHA-96008200).

* To whom correspondence should be addressed.

[1] Abbreviations: MCAD, human liver medium-chain acyl-CoA dehydrogenase; FAD, flavin adenine dinucleotide; OceCoA, 2-octenoyl coenzyme A; IPCoA, 3-indolepropionyl coenzyme A; IACoA, *trans*-3-indoleacryloyl coenzyme A; AcAc-CoA, acetoacetyl-CoA; $FcPF_6$, ferricenium hexafluorophosphate; ETF, electron-transferring flavoprotein; $\Delta G°$, standard free energy change; $\Delta H°$, standard enthalpy change; $\Delta S°$, standard entropy change; K_a, association constant; CT, charge-transfer; EDTA, ethylenediaminetetraacetic acid.

S0006-2960(98)00380-8 CCC: $15.00
Published on Web 05/22/1998

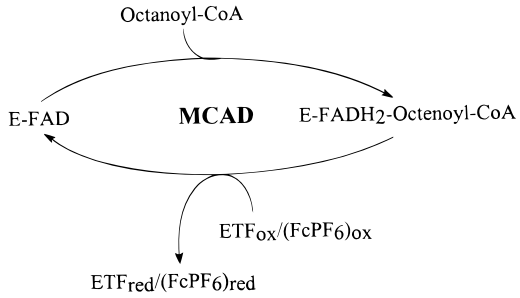

(2)

Contrary to the previous proposal, based on the X-ray crystallographic structures of pig liver MCAD in the absence and presence of C_8-CoA (*7*, *12*), we provided kinetic evidence that the binding of several CoA-ligands (including octenoyl-CoA) to the enzyme involved an obligatory change in the protein conformation (*5*, *8*, *9*, *13*, *14*). A similar conclusion was derived for the binding of acyl-CoAs to E−FAD followed by its concomitant reduction (*8*, *9*, *15*−*17*). All the transient kinetic data for the interaction of different CoA-ligands with the enzyme (*5*, *8*, *9*, *13*−*17*) led to the suggestion that the overall binding process was comprised of at least two consecutive steps (eq 3).

$$\text{E}-\text{FAD} + \text{ligand} \underset{K_L}{\rightleftharpoons} \text{E}-\text{FAD}-\text{ligand} \overset{k_2}{\underset{k_{-2}}{\rightleftharpoons}} (\text{E}-\text{FAD}-\text{ligand})^* \quad (3)$$

The first (fast) step involves a simple association of the ligand to the enzyme (with a dissociation constant of K_L), without yielding any spectral changes of the enzyme-bound FAD and/or of the ligand (*5*, *14*, *18*−*20*). The resultant complex is formalistically referred to as the collision or Michaelis complex. The latter complex undergoes a slow isomerization reaction (with forward and reverse rate constants of k_2 and k_{-2}, respectively) with a concomitant change in the electronic structures of the enzyme-bound FAD and the ligand (represented by an asterisk). The spectrally distinct form of the E−FAD−ligand complex is referred to as the isomerized complex (*5*, *14*, *18*−*20*).

In attempting to discern the structural−functional aspects of the MCAD-catalyzed reaction, we resorted to employing site-specific mutations, particularly at the active site region of the enzyme, and undertaking comparative studies between the wild-type and the mutant enzymes (*21*). We recently characterized a mutation, in which the active site residue Glu-376 was replaced by Asp, from the point of view of the efficiency of proton transfer from acyl-CoA substrates. A comparative account of the experimental data between the wild-type and E376D mutant enzyme revealed the following consequences of the above mutation (*21*): (A) The steady-state rates of both octanoyl-CoA- and indolepropionyl-CoA (IPCoA)-dependent reactions were impaired by 15−20-fold, and there was no selective solvent deuterium isotope effect on the enzyme catalysis. (B) The rate of inactivation of the enzyme by 2-octynoyl-CoA (known to proceed via abstraction of the γ-proton; *22*) was impaired by about 15-fold. (C) The rate-limiting step of the octanoyl-CoA-dependent reaction was changed from the product dissociation step (in the case of the wild-type enzyme) to the flavin reduction step (*8*, *9*, *23*). (D) The previously noted synergism between the rates of the octanoyl-CoA-dependent reductive half-reaction of the enzyme and the enzyme−octenoyl-CoA interaction was abolished (8, 14).

The question arose whether the deletion of a methylene group from the side chain of Glu-376 (upon Glu-376→Asp mutation) only affected the properties related to proton transfer (due to increase in the distance separating the proton donor and acceptor residues; *21*), or it also had influence on the conformation of the enzyme protein. The latter was important since the excised methylene group would be expected to create a "void" in the vicinity of the enzyme active site (*24*), and if such a void was not filled by a water molecule, the neighboring amino acid residues would move to fill in the vacant space. Although such movements may not be substantial to induce global changes in the protein conformation, they may just be adequate to influence the distance separating the CoA-ligands and the isoalloxazine ring of the enzyme-bound FAD, and thus in turn affects the spectral, thermodynamic, and kinetic properties of the enzyme−ligand complexes. The latter seemed to be corroborated by the fact that the E376D mutation altered the electronic spectrum of the enzyme-bound IACoA, and their associated thermodynamic and kinetic properties (our unpublished results).

We deliberated whether the native structure of the (E376D) mutant enzyme (which was presumably stabilized following the readjustment of the side chain residues around the putative void) was further readjusted upon binding of a CoA-ligand, and if so, in what respect(s) the mutant enzyme−ligand complexes differ from the wild-type enzyme−ligand complexes. Aside from these, we considered whether the above differences were ligand-specific. With these points in mind, we decided to compare the spectral, thermodynamic, and kinetic properties for the interactions of structurally different types of CoA-ligands, viz., octenoyl-CoA, acetoacetyl-CoA, and IACoA, upon binding to the oxidized forms of the wild-type and E376D mutant enzymes.

MATERIALS AND METHODS

Materials. Acetoacetyl-CoA, octanoyl-CoA, and EDTA were purchased from Sigma. Indolepropionic acid and *trans*-3-indoleacrylic acid were purchased from Aldrich. Octenoic acid was purchased from Pfaltz and Bauer. All other reagents were of analytical grade.

Methods. Unless stated otherwise, all experiments were conducted at 25 °C in 50 mM potassium phosphate buffer (pH 7.6) containing 0.3 mM EDTA, 10% glycerol, and 100 mM KCl. The site-specific mutation of the active site residue Glu-376 to Asp (E376D) in human liver medium-chain acyl-CoA dehydrogenase (MCAD) was performed as described previously (*21*). The wild-type and E376D mutant enzymes were expressed and purified according to Peterson et al. (*14*, *21*), and assayed by monitoring the reduction of ferricenium hexafluorophosphate ($FcPF_6$) at 300 nm ($\epsilon_{300} = 4.3$ mM^{-1} cm^{-1}; *22*) in a reaction mixture containing 100 μM octanoyl-CoA and 350 μM $FcPF_6$. Since the wild-type and E376D mutant enzymes had an isosbestic point at 446 nm, their concentrations were determined using the extinction coefficient of 15.4 mM^{-1} cm^{-1} at 446 nm (*25*).

The CoA derivatives 3-indolepropionyl-CoA (IPCoA), *trans*-3-indoleacryloyl-CoA (IACoA), and 2-octenoyl-CoA were synthesized by the mixed anhydride procedure of

Bernert and Sprecher (*26*) as described previously (*5*, *14*). The concentrations of IPCoA, IACoA, and 2-octenoyl-CoA were determined using their extinction coefficients of 18.2, 26.5, and 20.4 mM^{-1} cm^{-1} at 259, 367, and 258 nm, respectively (*8*, *14*).

Spectrophotometric Titrations of the Wild-Type and E376D Mutant MCADs by Selected Ligands. The spectrophotometric titrations of wild-type and E376D mutant enzymes by selected ligands, namely, octenoyl-CoA, acetoacetyl-CoA, and IACoA, were performed either on a Beckman-7400 diode array spectrophotometer or on a Perkin-Elmer lambda-3B spectrophotometer. The difference spectra of the enzyme−ligand complexes were generated by subtracting the spectra of the individual components from their mixture (after dilution corrections). The binding isotherms for the interactions of different ligands to the wild-type and E376D mutants were constructed by spectrophotometric titrations of the enzymes by their cognate ligands at specific wavelengths. The dissociation constants and the overall amplitudes of the absorption changes during such titrations were discerned by analyzing the experimental data by a complete solution of the quadratic equation describing the enzyme−ligand interaction (*27*).

Transient Kinetic Experiments. The single-wavelength transient kinetic experiments were performed on an Applied Photophysics SX-17 MV stopped-flow system (optical path length 10 mm, dead time 1.3−1.5 ms). Depending on the type of experiment, the stopped-flow was configured in either a single or a sequential mixing mode. In the single mixing mode, the contents of syringes A and B were diluted by 50%, whereas in the sequential mixing mode, the contents of both syringes were diluted by 75% and the content of syringe C was diluted by 50%. The stopped-flow kinetic traces were analyzed by the data analysis package provided by Applied Photophysics.

The rate constants for the association of different CoA-ligands to the wild-type and E376D mutant enzymes were determined by mixing the above species via the stopped-flow syringes (under pseudo-first-order conditions: [E−FAD] $\ll$ [ligand]), and monitoring the time-dependent absorption changes at specific wavelengths. The rate constants for the dissociation of ligands from their respective enzyme sites were determined by the octanoyl-CoA or acetoacetyl-CoA displacement methods as described by Kumar and Srivastava (*9*) and by Johnson et al. (*5*).

Isothermal Titration Microcalorimetry. The isothermal microcalorimetric experiments were performed on a MCS isothermal titration calorimeter (ITC) from Microcal Inc., as described by Srivastava et al. (*28*). The sample cell was filled with 1.8 mL of the buffer (control) or enzyme solution (effective volume = 1.36 mL). The injector was filled with 250 μL of the ligand. The titration was initiated by the first (preliminary) injection of 1 μL, followed by 60 injections (4 μL each) of the ligand. During the experiment, the enzyme solution was stirred at a constant rate of 400 rpm. The enzyme concentration was adjusted by 2% to allow for dilution following a buffer rinse of the cell.

All of the calorimetric data were presented after correction for the background. Since the titration produced small turbidity in the enzyme solution, the background heat was slightly larger than that obtained during the control experiment. Hence, the heat produced at the end of titration (where the enzyme was saturated by the ligand) was taken as the measure of the background heat. The experimental data were analyzed according to Wiseman et al. (*29*).

The data analysis produced three parameters, viz., stoichiometry (n), association constant (K_a), and the standard enthalpy changes ($\Delta H°$) for binding of the ligands to MCAD. The standard free energy change ($\Delta G°$) for the binding was calculated according to the relationship: $\Delta G° = -RT \ln K_a$. Given the magnitudes of $\Delta G°$ and $\Delta H°$, the standard entropy change ($\Delta S°$) for the binding process was calculated according to the standard thermodynamic equation: $\Delta G° = \Delta H° - T\Delta S°$.

Molecular Model-Building Studies. All the molecular model building studies were performed on a Silicon Graphics-O2 molecular modeling workstation, with the aids of Insight-II (97), Biopolymers, Homology-97, and Discover-97 softwares, developed by Molecular Simulations, Inc. The coordinates for the X-ray crystallographic structure of pig liver medium-chain acyl-CoA dehydrogenase in the presence of C_8-CoA, contained in the file 3MDE, were downloaded from the Brookhaven Protein Data Bank. The ω end of the enzyme-bound C_8-CoA structure was differently modified to adopt the structures of indoleacryloyl-CoA or acetoacetyl-CoA by the help of the Biopolymer module of Insight-II. The glutamate-376→Asp mutation was constructed by replacing the side chain of Glu-376 by Asp by aid of Homology-97 software.

The individual wild-type and E376D mutant−ligand structures were subjected to the energy minimization using the consistent valence force field (CVFF) by the aid of Discover-97 software (*30*). Prior to minimization, one subunit of the enzyme (along with the water molecules within 4 Å interface) was isolated, the bond orders of both FAD and CoA-ligands were set, and the hydrogens were added to both protein and ligands at the neutral pH. The energy minimization was performed using a combination of the steepest descent and conjugate gradient approach, via the following sequence of steps: (A) By fixing all atoms, except for hydrogen, the appropriate structure was subjected to 200 iterations of steepest descent followed by 100 iterations of conjugate gradient until a derivative of 1 kcal mol^{-1} $Å^{-1}$ was achieved. (B) By fixing the protein backbone, and FAD and CoA-ligands, 2000 iterations were performed via the above minimization steps until a derivative of 0.01 kcal mol^{-1} $Å^{-1}$ was achieved. (C) Finally, by restraining the backbone structure, the energy minimization (15 000 iterations) was performed via the conjugate gradient approach until a derivative in the range of 10^{-4}−10^{-5} kcal mol^{-1} $Å^{-1}$ was achieved.

Strategically, the wild-type ligand structure was first minimized, and after creating the mutation in the minimized structure, the resultant structure was subjected to further minimization via the above sequence of steps.

It should be mentioned that when the hydrogen atoms were added to the protein structure, the hydrogen of the 2′-ribityl hydroxyl group of FAD formed a hydrogen bond to its neighboring 3′-hydroxyl oxygen. When this arrangement was left as such, the minimized structure attained a maximum derivative in the range of 0.4−1 kcal mol^{-1} $Å^{-1}$. However, when the above hydrogen bond was manually broken, and the corresponding bond was rotated such that it formed a new hydrogen bond with the carbonyl oxygen of the CoA-

ligand (as expected for the polarization of the carbonyl group of the CoA-ligands), the maximum derivative of the minimized structure decreased to a level of $10^{-4}-10^{-5}$ kcal mol^{-1} Å^{-1}. The latter values are considered to be fairly low for the globally minimized structure of protein−ligand complexes in general (*31*).

RESULTS

We investigated the effect of Glu-376→Asp (E376D) mutation on the spectral, thermodynamic, and kinetic properties for the binding of structurally different types of CoA-ligands, namely, octenoyl-CoA, acetoacetyl-CoA, and indoleacryloyl-CoA (IACoA), to the oxidized form of human liver medium-chain acyl-CoA dehydrogenase (MCAD).

Influence of the E376D Mutation on the Spectral Properties and Binding Constants of the Enzyme−Ligand Complexes. The binding of octenoyl-CoA, acetoacetyl-CoA, and indoleacryloyl-CoA to the oxidized form of MCAD exhibits different types of spectral changes in the UV/visible region (*5*, *8*, *9*, *14*, *32*). Whereas the binding of octenoyl-CoA to the enzyme is characterized by a small red shift in the electronic spectrum of the enzyme-bound FAD, both around 370 and 450 nm regions with concomitant emergence of a shoulder band around 490 nm, the binding of acetoacetyl-CoA is primarily characterized by the emergence of a pronounced charge-transfer complex band around 545 nm (*8, 9, 14*). Unlike these, the electronic spectrum of the enzyme-bound IACoA is dominated by a marked increase and decrease in the spectral bands at 416 and 358 nm, respectively (*5*). These spectral changes with individual CoA-ligands are best characterized by the difference spectra, i.e., the spectra of the mixture minus the individual components.

Figure 1 shows the difference spectra of the MCAD−ligand complexes, involving both wild-type and E376D mutant enzymes, and octenoyl-CoA (panel A), acetoacetyl-CoA (panel B), and IACoA (panel C) as selected CoA-ligands. All these spectra were generated by incubating nearly saturating concentrations of the individual ligands to the wild-type and E376D mutant enzymes, followed by subtracting the contributions of the individual components (after appropriate dilution corrections). A casual comparison of the spectral data of Figure 1 reveals that although the E376D mutation does not affect the position of the characteristic spectral peaks of the individual enzyme−ligand complexes, it influences the amplitudes of such peaks, albeit to different extents with different ligands. In the case of octenoyl-CoA (Figure 1, panel A), the E376D mutation exhibits a negligible effect on the resultant spectral peaks of the enzyme−octenoyl-CoA complex. On the other hand, in the case of acetoacetyl-CoA, the E376D mutation decreases the amplitude of charge-transfer band (contributed by the anionic form of acetoacetyl-CoA being the electron donor and the enzyme-bound FAD being the electron acceptor) at 546 nm by 1.8-fold. In contrast to these, in the case of IACoA, the above mutation increases the amplitudes of the absorption bands both at 416 nm and at 358 nm by 2.7- and 2.9-fold, respectively.

To ascertain whether the amplitudes of the spectral changes of Figure 1 were due to ligand-specific alteration in the binding constants of the respective enzyme−ligand com-

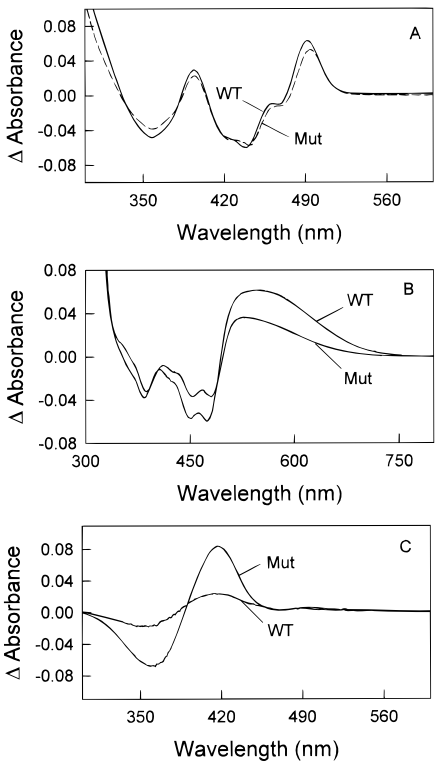

FIGURE 1: UV/visible difference spectra for the interactions of different CoA-ligands with the wild-type and Glu-376→Asp mutant medium-chain acyl-CoA dehydrogenases (MCADs). Panels A, B, and C contain the spectral data for the interaction of octenoyl-CoA, acetoacetyl-CoA, and IACoA with the wild-type (WT) and mutant (Mut) enzymes. The experimental procedures are described under Materials and Methods. The concentrations of enzymes and CoA-ligands for the spectral data of different panels were as follows. Panel A: [WT or Mut] = 20 μM, [octenoyl-CoA] = 54.4 μM. Panel B: [WT or Mut] = 20 μM, [acetoacetyl-CoA] = 245.7 μM. Panel C: [WT or Mut] = 5 μM, [IACoA] = 27.9 μM.

plexes, we titrated fixed concentrations of the wild-type and mutant enzymes with increasing concentrations of the individual ligands. Such titrations were performed at 442, 545, and 416 nm involving octenoyl-CoA, acetoacetyl-CoA, and IACoA, respectively. A comparative account of the binding isotherms for the interactions of the above ligands to the wild-type and E376D mutant enzymes is shown in Figure 2. The solid smooth lines are the best fit of the experimental data according to the classical quadratic equation for one-step enzyme−ligand interaction (*27*). The magnitudes of the dissociation constants and the total absorption changes at corresponding wavelengths (at which the titrations were performed), derived from the analysis of the experimental data, are summarized in Table 1.

From the data of Table 1, it is evident that whereas the dissociation constant of octenoyl-CoA from the enzyme−octenoyl-CoA complex was essentially unaffected, the dissociation constants of acetoacetyl-CoA and IACoA from their corresponding enzyme sites increased and decreased by 3-fold and 4-fold, respectively, upon Glu-376→Asp mutation. In addition, the above mutation exhibited a miniscule effect, decreased, and increased the total amplitude of the absorption changes involving octenoyl-CoA, acetoacetyl-CoA, and IACoA, respectively.

With the precedents of our earlier findings, it appeared evident that the above observations had a common molecular origin (*5*, *8*, *9*, *14*). With all the above CoA-ligands, we

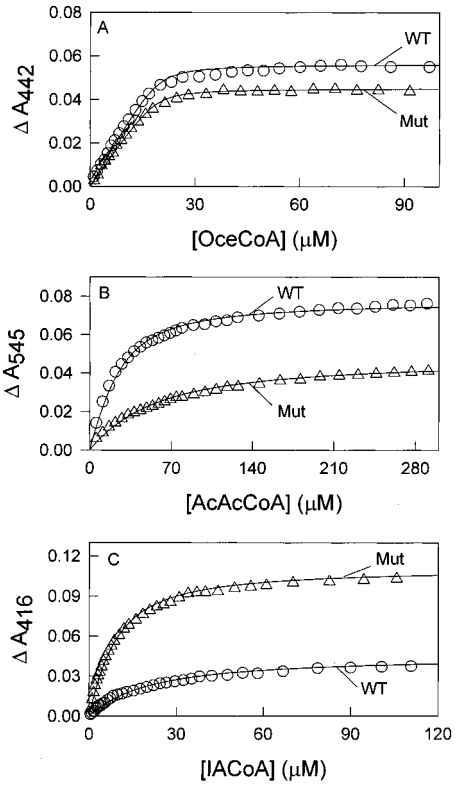

FIGURE 2: Binding isotherms for the interactions of CoA-ligands with the wild-type and Glu-376→Asp mutant MCADs. The titration results of fixed concentrations of wild-type (WT) and mutant (Mut) enzymes by increasing concentrations of octenoyl-CoA, acetoacetyl-CoA, and IACoA are shown in panels A, B, and C, respectively. The concentrations of the wild-type and mutant enzymes for the data of panels A, B, and C were 20 μM, 20 μM, and 5 μM, respectively. The wavelengths of the above titrations (denoted by ΔA_λ on the *y*-axis) were 442, 545, and 416 nm, respectively. The experimental data for the wild-type and mutant enzymes are represented by open circles and open triangles, respectively. The solid smooth lines are the best fit of the experimental data by the classical quadratic equation for the enzyme−ligand interactions. The magnitudes of the dissociation constants (K_d) and the amplitudes for the binding of individual ligands to the wild-type and mutant enzymes are summarized in Table 1.

Table 1: Summary of the Ligand Binding Studies via the Spectrophotometric Method[a]

enzyme	ligand[b]	K_d (μM)	Δ Absorbance
wild-type	OceCoA	0.67 ± 0.1	0.056 ± 0.002
	AcAcCoA	12.3 ± 0.7	0.077 ± 0.002
	IACoA	17.9 ± 1.3	0.039 ± 0.004
E376D	OceCoA	0.61 ± 0.2	0.045 ± 0.003
	AcAcCoA	44.7 ± 2.1	0.042 ± 0.003
	IACoA	4.5 ± 0.4	0.103 ± 0.002

[a] Derived from the data of Figure 2. [b] OceCoA, AcAcCoA, and IACoA refer to octenoyl-CoA, acetoacetyl-CoA, and indoleacryloyl-CoA, respectively.

previously provided evidence that the spectral changes upon formation of the individual enzyme−ligand complexes originated upon isomerization of their cognate collision complexes (see eq 3), and the latter step served as the major contributor to the overall dissociation constants of the enzyme−ligand complexes. Hence, any factor that increased the isomerization equilibrium (i.e., the ratio of k_2 to k_{-2}) was found to increase the total amplitude of the binding isotherm, and decrease the dissociation constant parameter (*18*, *20*, *33*).

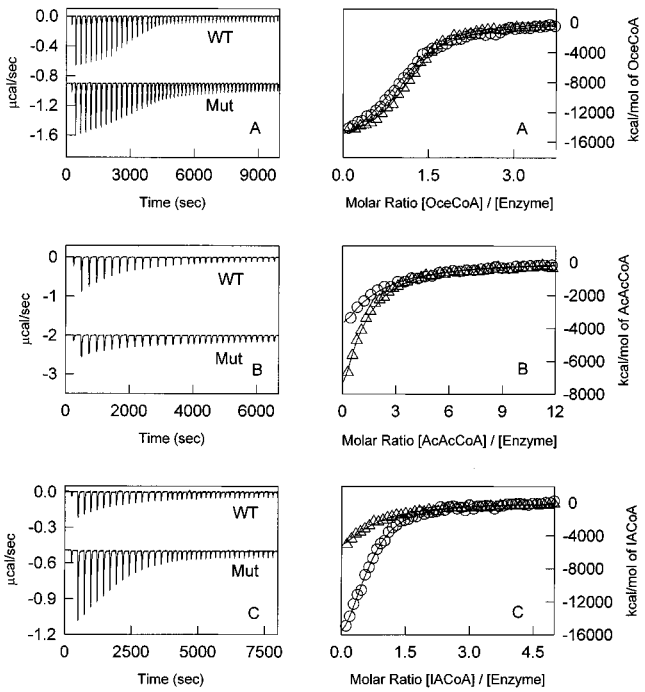

FIGURE 3: Isothermal microcalorimetric titration data for the interactions of CoA-ligands with the wild-type and Glu-376→Asp mutant MCADs. The titration results for the binding of octenoyl-CoA, acetoacetyl-CoA, and IACoA to the wild-type (WT) and mutant (Mut) enzymes are shown in panels A, B, and C, respectively. Whereas the left panels show the raw calorimetric data, the right panels show the relationship between the amount of heat produced per mole of ligand to the molar ratio of ligand to enzyme. The experimental data for the wild-type and mutant enzymes are represented by open triangles and open circles, respectively. The concentration of wild-type and E376D mutant enzyme was fixed at 10 μM for all titrations. The stock concentrations of octenoyl-CoA, acetoacetyl-CoA, and IACoA were 300 μM, 1.2 mM, 450 μM, respectively. The solid smooth lines are the best fit of the experimental data according to Wiseman et al. (29). The magnitudes of stoichiometry (*n*), the association constant for the enzyme−ligand complex (K_a), and the standard enthalpic changes ($\Delta H°$) derived from the best fit of the experimental data are summarized in Table 2.

Influence of the E376D Mutation on the Thermodynamic Properties of the Enzyme−Ligand Complexes. To ascertain the thermodynamic contributions of the E376D mutation on the binding of the above ligands to MCAD, we resorted to the isothermal microcalorimetric titration method. We previously reported that whereas the binding of octenoyl-CoA to pig kidney MCAD was predominantly enthalpically driven (*28*), the binding of IACoA to the pig kidney enzyme was favored almost equally by both enthalpic and entropic contributions (*27*). A detailed thermodynamic study for the binding of octenoyl-CoA and IACoA to human liver MCAD, from the point of view of marked differences between the enzyme site environments of the pig kidney and human liver enzymes, will be published subsequently.

Figure 3 shows comparative microcalorimetric titration profiles for the binding of octenoyl-CoA, acetoacetyl-CoA, and IACoA to the wild-type and E376D mutant enzymes. The left panels show the raw calorimetric data for the titration of either 10 μM wild-type or E376D mutant enzyme by 60 4-μL injections (except for the first injection which was 1 μL) of individual CoA-ligands. The data in panels A, B, and C represent the titration results of the wild-type and E376D mutant enzymes by octenoyl-CoA, acetoacetyl-CoA,

Table 2: Summary of the Isothermal Titration Microcalorimetric Studies[a]

enzyme	ligand	T (K)	n	K_a (M^{-1})	$\Delta H°$ (kcal/mol)	$\Delta G°$ (kcal/mol)	$T\Delta S°$ (kcal/mol)
wild-type	OceCoA	298.2	1.02 ± 0.01	$(9.94 \pm 0.5) \times 10^5$	-17.9 ± 0.2	-8.2 ± 0.4	-9.7
	AcAcCoA	298.3	0.6 ± 0.03	$(6.56 \pm 0.2) \times 10^4$	-29.2 ± 0.3	-6.6 ± 0.2	-22.6
	IACoA	298.2	0.48 ± 0.02	$(6.22 \pm 0.2) \times 10^4$	-15.9 ± 0.2	-6.5 ± 0.3	-9.4
E376D	OceCoA	298.2	1.07 ± 0.01	$(5.41 \pm 0.2) \times 10^5$	-17.3 ± 0.1	-7.8 ± 0.3	-9.5
	AcAcCoA	298.2	0.6 ± 0.03	$(3.2 \pm 0.9) \times 10^4$	-23.6 ± 0.4	-6.1 ± 0.1	-17.5
	IACoA	298.2	0.62 ± 0.01	$(4.02 \pm 0.2) \times 10^5$	-22.3 ± 0.6	-7.60 ± 0.4	-14.7

[a] Derived from the analysis of the experimental data of Figure 3.

and IACoA, respectively. The stock concentrations of these ligands were 300 μM, 1.2 mM, and 400 μM, respectively. For clarity, the raw calorimetric data (left panels) of the mutant enzyme have been arbitrarily offset. An examination of the data in the left panels suggests the titration amplitudes (which serve as a qualitative measure of the enthalpic changes) between the wild-type and the mutant enzymes are ligand-dependent. For example, in the case of octenoyl-CoA, the titration amplitude appears to be same with both wild-type and mutant enzymes. On the other hand, in the case of acetoacetyl-CoA, the titration amplitude is higher with wild-type enzyme, and in the case of IACoA, it is higher with the mutant enzyme. Note that the latter trend is qualitatively similar to the spectral changes (Figure 1) and the dissociation constants (Figure 2 and Table 1) of the corresponding enzyme−ligand complexes.

The right panels (A, B, and C) of Figure 3 are the calculated results, derived from the corresponding raw calorimetric data of the left panels. The amount of heat evolved (calculated from the area of the individual peak) per mole of ligand as a function of the molar ratio of the ligand to the enzyme is plotted. The titration results for the wild-type and mutant enzymes are represented by open triangles and open circles, respectively. The solid smooth lines are the best fit of the experimental data for a single enzyme−ligand binding site model according to Wiseman et al. (*29*). Such analyses yielded the stoichiometry (n), association constant (K_a), and enthalpic changes ($\Delta H°$) for the binding of individual ligands to both wild-type and mutant enzymes. The K_a values thus determined were translated into the standard free energy changes ($\Delta G°$) according to the standard thermodynamic relationship: $\Delta G° = -RT \ln (K_a)$. Given the $\Delta G°$ and $\Delta H°$ values for the binding of individual CoA-ligands to the wild-type and E376D mutant enzymes, the entropic contributions ($T\Delta S°$) were determined ($\Delta G° = \Delta H° - T\Delta S°$). These thermodynamic parameters are summarized in Table 2.

On examination of the data of Table 2, it is clear that whereas the $\Delta H°$ value for the binding of octenoyl-CoA to the enzyme is not much affected upon Glu-376→Asp mutation, it is drastically affected for the binding of acetoacetyl-CoA and IACoA to the enzyme, albeit in an opposite manner. In the case of acetoacetyl-CoA, the E376D mutation results in an increase in the $\Delta H°$ value (i.e., causing the overall binding process to be enthalpically less favorable) by about 5.6 kcal/mol. On the contrary, in the case of IACoA, the $\Delta H°$ value decreases (i.e., becomes more favorable) by 6.4 kcal/mol by the above mutation. Since the $\Delta G°$ values for the binding of either of the above ligands are not substantially affected by the above mutation, it follows that the $\Delta H°$ and $T\Delta S^0$ values are mutually compensated. This is clearly apparent by the fact that the $T\Delta S°$ values for the binding of acetoacetyl-CoA and IACoA to the wild-type enzyme are 5.1 and 5.3 kcal/mol less and more favorable, respectively, as compared to the E376D mutant enzyme.

Influence of the E376D Mutation on the Association and Dissociation Kinetics. The characteristic spectral signals for the interactions of different CoA-ligands to the wild-type and E376D mutant enzymes (Figure 1) enabled us to investigate their association and dissociation kinetics. Figure 4 shows the time courses for the enzyme−ligand interactions (monitored at specific wavelengths) upon mixing the wild-type and E376D mutant enzymes with high and saturating concentrations of the individual ligands (under pseudo-first-order conditions: [E] ≪ [ligand]) via the stopped-flow syringes. The wavelengths for monitoring the interactions of octenoyl-CoA (panel A), acetoacetyl-CoA (panel B), and IACoA (panel C) were 442, 545, and 416 nm, respectively. Whereas the reaction traces for the interactions of octenoyl-CoA and acetoacetyl-CoA were best fitted by the double-exponential rate equation, the reaction trace for the interaction of IACoA was best fitted by the single-exponential rate equation. The solid smooth lines are the best fit of the experimental data for biphasic (panels A and B) and single-exponential (panel C) rate equations, respectively. The derived rate constants and amplitudes of the individual traces are contained in the figure legend. It should be mentioned that the kinetic profile for the association of acetoacetyl-CoA to pig kidney MCAD was repeatedly found to be single-exponential instead of biphasic in nature (*8*, *9*). No such discrepancy was found for the interaction of either octenoyl-CoA or IACoA to pig kidney and human liver enzymes. We do not understand, at this time, the molecular basis of the above discrepancy.

On comparison of the association reaction traces of Figure 4, it is apparent that except for the difference in the amplitudes, the relaxation rate constants are not much different (for either of the above ligands) between the wild-type and E376D mutant enzymes. The difference in the amplitude is merely due to the previously noted influence (see Figure 1) of Glu-376→Asp mutation on the spectral properties of the enzyme−ligand complexes. Hence, the experimental data of Figure 4 suggest that the relaxation rate constants for the association of different ligands to the enzyme are not affected by the E376D mutation.

The similarity in the association rates of different ligands between the wild-type and E376D mutant enzymes was surprising, particularly since the overall equilibrium constants for the association of different ligands to the enzymes were affected by the E376D mutation (see Figure 2 and Table 1). However, on consideration that the overall equilibrium constant was comprised of both forward and reverse (isomerization) steps, we proceeded to determine the dissociation

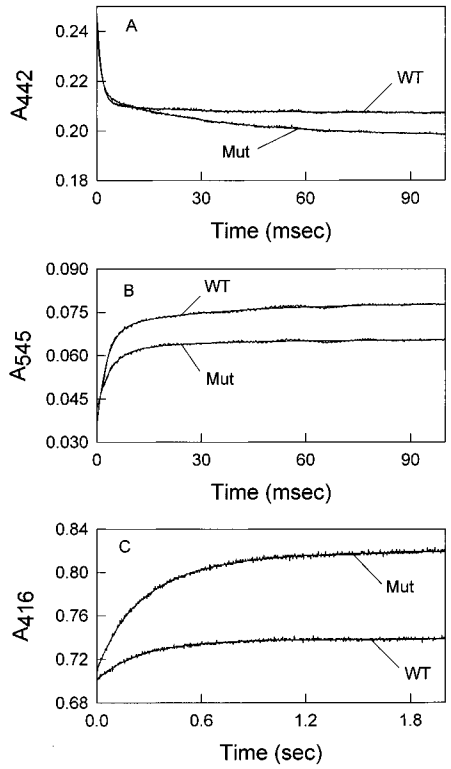

FIGURE 4: Transient kinetics for the interaction of CoA-ligands with the wild-type and Glu-376→Asp mutant enzymes. The stopped-flow traces for the interactions of octenoyl-CoA (5 °C), acetoacetyl-CoA, and IACoA with the wild-type (WT) and mutant (Mut) enzymes are shown in panels A, B, and C, respectively. The wavelengths for monitoring the above interactions were 442, 545, and 416 nm, respectively. The solid smooth lines are the best fit of the experimental data of panels A and B according to the biphasic rate equation, and those of panel C by the single-exponential rate equation. The (after mixing) concentrations of enzyme and CoA-ligands, the fast ($1/\tau_f$) and slow ($1/\tau_s$) relaxation rate constants for the biphasic fit (panels A and B), and the $1/\tau$ for the single-exponential fit (panel C) of the experimental data, and their associated amplitudes are summarized as follows: Panel A: [WT or Mut] = 15 μM, [octenoyl-CoA] = 150 μM, $1/\tau_f = 842.7 \pm 19.9$ s^{-1}, $\Delta A_f = 0.043 \pm 0.001$, $1/\tau_s = 72.3 \pm 2.5$ s^{-1}, $\Delta A_s = 0.004 \pm 0.0001$ (wild-type enzyme); and $1/\tau_f = 753.2 \pm 20.3$ s^{-1}, $\Delta A_f = 0.027 \pm 0.00008$, $1/\tau_s = 29.8 \pm 0.3$ s^{-1}, $\Delta A_s = 0.016 \pm 0.00005$ (mutant enzyme). Panel B: [WT or Mut] = 20 μM, [acetoacetyl-CoA] = 1 mM, $1/\tau_f = 353.4 \pm 5.5$ s^{-1}, $\Delta A_f = 0.034 \pm 0.0003$, $1/\tau_s = 30.7 \pm 1.0$ s^{-1}, $\Delta A_s = 0.009 \pm 0.0001$ (wild-type enzyme); and $1/\tau_f = 272.4 \pm 6.9$ s^{-1}, $\Delta A_f = 0.020 \pm 0.0003$, $1/\tau_s = 44.3 \pm 2.2$ s^{-1}, $\Delta A_s = 0.004 \pm 0.0002$ (mutant enzyme). Panel C: [WT or Mut] = 5 μM, [IACoA] = 200 μM, $1/\tau = 3.72 \pm 0.04$ s^{-1}, $\Delta A = 0.036 \pm 0.0002$ (wild-type enzyme); and $1/\tau = 3.27 \pm 0.02$ s^{-1}, $\Delta A = 0.103 \pm 0.0003$ (mutant enzyme).

"off-rates" of the individual ligands from the wild-type and the mutant enzyme sites. In this endeavor, we employed our previously developed ligand displacement methods (*5*, *8*, *9*). For measuring the dissociation off-rates of octenoyl-CoA and IACoA from the wild-type and E376D mutant enzymes, we mixed appropriate enzyme−ligand complexes with a high concentration of acetoacetyl-CoA via the stopped-flow syringes, followed by recording the time-dependent absorption changes at 545 and 416 nm, respectively. However, in the case of acetoacetyl-CoA, the displacing ligand was octenoyl-CoA, and during this process, the time course for the decrease in absorption was once again monitored at 545 nm. Due to technical problems noted previously (*8*), the off-rate measurements involving octenoyl-CoA were performed by the double mixing approach.

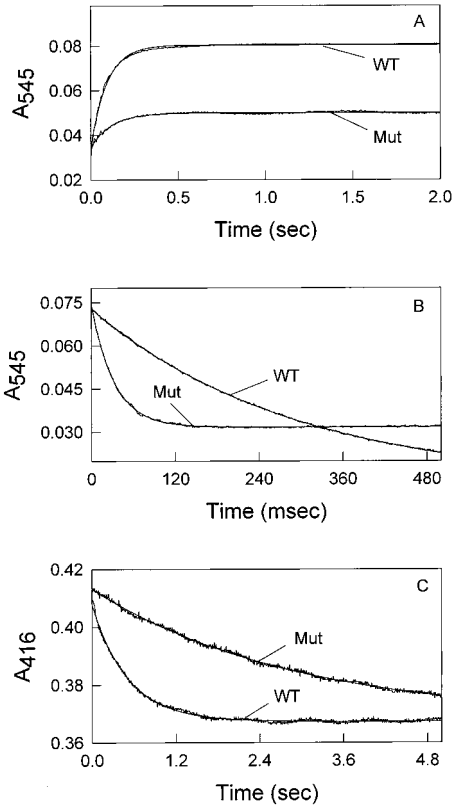

FIGURE 5: Dissociation off-rates of the CoA-ligands from wild-type and Glu-376→Asp mutant MCADs. The time courses for the dissociation of octenoyl-CoA, acetoacetyl-CoA, and IACoA from the oxidized forms of the wild-type (WT) and mutant (Mut) enzymes are shown in panels A, B, and C, respectively. Whereas the dissociation off-rates of octenoyl-CoA (panel A) and IACoA (panel C) were measured by the acetoacetyl-CoA displacement method, the dissociation off-rate of acetoacetyl-CoA (panel B) was measured by the octenoyl-CoA displacement. The data of panel A were obtained via the double-mixing stopped-flow method. The reaction traces of Panels A and B were obtained at 545 nm, and those of panel C were obtained at 416 nm. The solid smooth lines are the best fit of the experimental data (of each panel) by a single-exponential rate equation. The after-mixing concentrations of the individual components, the derived rate constants, and the amplitudes for the data of the individual panels are summarized as follows: Panel A: [WT or Mut] = 20 μM, [octenoyl-CoA] = 20 μM, [acetoacetyl-CoA] = 1 mM, $1/\tau = 10.7 \pm 0.1$ s^{-1}, $\Delta A_{545} = 0.047 \pm 0.0002$ (wild-type enzyme); and $1/\tau = 8.6 \pm 0.1$ s^{-1} $\Delta A_{545} = 0.016 \pm 0.0001$ (mutant enzyme). Panel B: [WT or Mut] = 20 μM, [acetoacetyl-CoA] = 0.5 mM, [octenoyl-CoA] = 0.8 mM, $1/\tau = 3.4 \pm 0.0086$ s^{-1}, $\Delta A_{545} = 0.061 \pm 0.00006$ (wild-type enzyme); and $1/\tau = 31.0 \pm 0.08$ s^{-1}, $\Delta A_{545} = 0.043 \pm 0.00007$ (mutant enzyme). Panel C: [WT or Mut] = 5 μM, [IACoA] = 50 μM, [acetoacetyl-CoA] = 1 mM, $1/\tau = 1.95 \pm 0.01$ s^{-1}, $\Delta A_{416} = 0.04 \pm 0.0001$ (wild-type enzyme); $1/\tau = 0.34 \pm 0.003$ s^{-1}, $\Delta A_{416} = 0.045 \pm 0.0002$ (mutant enzyme).

Figure 5 shows the comparative traces for dissociation of octenoyl-CoA (panel A), acetoacetyl-CoA (panel B), and IACoA (panel C) from the wild-type and E376D mutant enzyme sites. The solid smooth lines are the best fit of the experimental data for the single-exponential rate equation, with dissociation off-rate constants for octenoyl-CoA, acetoacetyl-CoA, and IACoA from the wild-type MCAD being 10.7 ± 0.1, 3.4 ± 0.009, and 1.95 ± 0.01 s^{-1}, respectively. The corresponding parameters for the E376D mutant enzyme were 8.6 ± 0.1, 31.0 ± 0.08, and 0.34 ± 0.003 s^{-1}, respectively. From these data, it is apparent that the

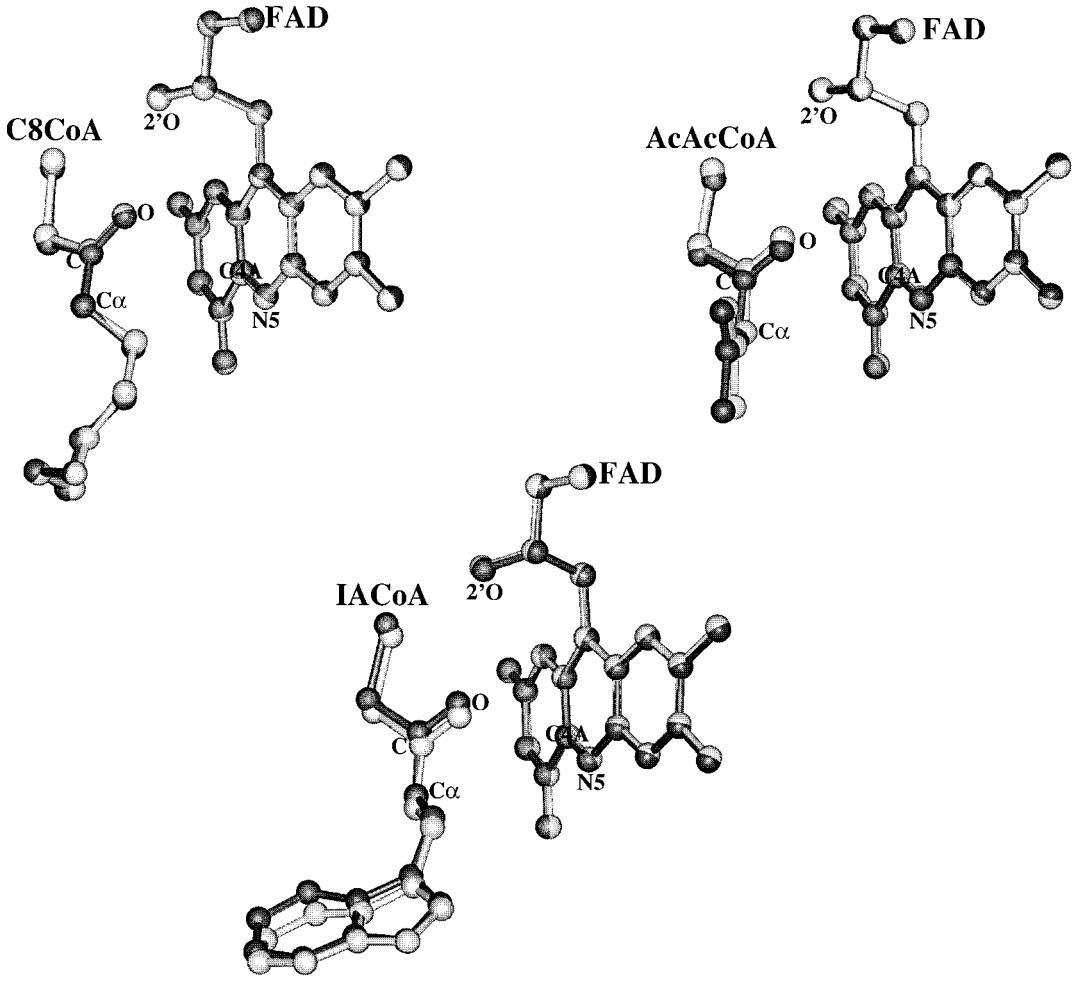

FIGURE 6: Spatial relationships of FAD and CoA-ligands, bound to the wild-type and Glu-376→Asp mutant MCAD structures. The light and dark colored ball-and-stick models of FAD and CoA-ligands represent their residence at the (energy-minimized) wild-type and mutant enzyme structures, respectively. For clarity, only part of the FAD and CoA-ligand structures is displayed, and the hydrogen atoms are deleted. Note that the Glu-376→Asp mutation does not alter the position of the isoalloxazine ring of FAD upon binding of either of the CoA-ligands to the enzyme sites. However, depending upon the type of CoA-ligand, the above mutation changes the position of the CoA-ligands. Unlike C_8-CoA, the carbonyl oxygen and C_α of acetoacetyl-CoA tend to move away from FAD, and the corresponding atoms of IACoA tend to move closer to FAD, upon Glu-376→Asp mutation.

dissociation off-rate of octenoyl-CoA from the enzyme site remains practically unaffected upon Glu-376→Asp mutation. On the contrary, the above mutation increases and decreases the dissociation off-rates of acetoacetyl-CoA and IACoA by about 9-fold and 6-fold, respectively. We previously established that with all these ligands, the dissociation off-rate constant qualitatively serves as a measure of k_{-2} of eq 3. Hence, without undergoing rigorous analyses of the association and dissociation parameters (as performed in our previous publications, *5*, *8*, *9*, *14*, *19*), it is qualitatively justifiable that the isomerization equilibrium (a qualitative measure of the ratio of k_2 to k_{-2} of eq 3) remains minimally affected, upon E376D mutation, in the case of octenoyl-CoA. The above isomerization equilibrium, on the other hand, decreases and increases (upon E376D mutation) in the case of acetoacetyl-CoA and IACoA, respectively. These qualitative conclusions are in accord with the observed quantitative differences in the binding parameters of the individual ligands derived from the spectroscopic (Table 1) and microcalorimetric (Table 2) titration results. Clearly, the experimentally observed differences in the spectroscopic, thermodynamic, and kinetic parameters for the binding of the above (structurally diverse ligands) to the wild-type and E376D mutant enzymes are primarily due to the ligand-specific alterations in the isomerization equilibrium of eq 3.

Molecular Modeling Studies. To discern the molecular basis of the above effects, we examined the influence of E376D mutation on the spatial relationships of enzyme-bound FAD and different CoA-ligands via the model-building studies. As described under Materials and Methods, the latter approach involved energy minimization of the individual wild-type enzyme−ligand complex structures, insertion of Glu-376→Asp mutation, and further minimization of the resultant mutant enzyme−ligand structures. The rms deviations (for the protein backbone) between the minimized wild-type and mutant structures containing different ligands were in the range of 0.007−0.28 Å. A comparison between the individual wild-type−ligand and mutant−ligand structures revealed that whereas Glu-376→Asp mutation did not alter the location of the enzyme-bound FAD, it slightly altered the location of the CoA-ligands. The rms deviations (for heavy atoms) of octenoyl-CoA, acetoacetyl-CoA, and IACoA between the wild-type and the mutant enzymes were found to be 0.091, 0.103, and 0.147 Å, respectively. Figure 6 depicts the spatial relationships between the enzyme-bound FAD and individual CoA ligands within the minimized wild-

Table 3: Selected Interatomic (Å) Distances between the Enzyme-Bound FAD and CoA-Ligands

interatomic distances	E−C_8 CoA	E−AcAcCoA	E−IACoA
wild-type MCAD			
C═O (CoA-ligand) and 2′-ribityl O (FAD)	2.94	3.79	3.55
C_α (CoA-ligand) and N5 (FAD)	4.37	4.27	4.27
C_α (CoA-ligand) and C4A (FAD)	5.11	5.22	5.24
E376D mutant MCAD			
C═O (CoA-ligand) and 2′-ribityl O (FAD)	3.03	4.04	3.22
C_α (CoA-ligand) and N5 (FAD)	4.38	4.49	4.18
C_α (CoA-ligand) and C4A (FAD)	5.11	5.42	5.16

type (light colored) and E376D mutant (dark colored) structures. Although all the CoA-ligands were found to be shifted (globally) from their original positions (upon E376D mutation), the distances between the carbonyl oxygen of the CoA-ligands and the 2′-ribityl hydroxyl group of FAD, and between the α-carbon atom of the CoA-ligands and C4A and N5 atoms of FAD, were found to be affected involving different CoA-ligands. From Figure 6 and Table 3, it is apparent that in the case of octenoyl-CoA, the E376D mutation does not alter the above distances. On the contrary, the above distances increase and decrease (upon E376D mutation) with acetoacetyl-CoA and IACoA ligands, respectively. The distance measurements (between selected atoms of FAD and CoA derivatives) summarized in Table 3 clearly reveal that whereas the E376D mutation increases the distance between the carbonyl oxygen of acetoacetyl-CoA and the 2′-ribityl oxygen of FAD by 0.24 Å, it decreases the distance between the carbonyl oxygen of IACoA and the 2′-ribityl oxygen of FAD by 0.33 Å, respectively. Unlike these, the distance separating the above atoms remained minimally affected (0.09 Å), upon E376D mutation, in the case of octenoyl-CoA. A qualitatively similar trend was found for the distance separating the α-carbon atoms of the individual ligands and the C4A and N5 atoms of FAD (see Table 3). As will be elaborated under Discussion, these distances are likely to be responsible for the spectral changes of the enzyme-bound FAD and/or the CoA-ligands within the enzyme site phase. Hence, it appears plausible that the discriminatory influence of Glu-376→Asp mutation on the spectral, thermodynamic, and kinetic properties for the binding of structurally different types of CoA-ligands to MCAD is mediated via the ligand-specific changes in certain interatomic distances between FAD and the CoA-ligands.

DISCUSSION

The experimental data presented in the previous section lead to the suggestion that Glu-376→Asp (E376D) mutation in MCAD exhibits discriminatory influence on the binding of selected CoA-analogues, viz., octenoyl-CoA, acetoacetyl-CoA, and indoleacryloyl-CoA (IACoA), to the oxidized form of the enzyme. This is supported by the following experimental evidence: (A) Whereas the E376D mutation practically does not influence the UV/visible spectral properties of the enzyme−octenoyl-CoA complex, it suppresses and enhances the spectral features of the enzyme−acetoacetyl-CoA and enzyme−IACoA complexes, respectively. (B) Whereas the E376D mutation does not influence the dissociation constant of the enzyme−octenoyl-CoA complex, it increases and decreases the dissociation constants of both the enzyme−acetoacetyl-CoA and the enzyme−IACoA complexes by about 3- and 4-fold, respectively (Figure 2 and Table 1). (C) Whereas the E376D mutation exhibits miniscule changes in the $\Delta H°$ value (e.g., by 0.6 kcal/mol) for the binding of octenoyl-CoA to the enzyme, it increases and decreases the above parameter for the binding of acetoacetyl-CoA and IACoA to the enzyme by 5.6 and 6.4 kcal/mol, respectively (Figure 3 and Table 2). (D) Whereas the E376D mutation exhibits practically no effect on the dissociation off-rate of octenoyl-CoA from the enzyme−octenoyl-CoA complex, it increases and decreases the above parameter of acetoacetyl-CoA and IACoA from their corresponding enzyme sites by 9-fold and 6-fold, respectively (Figure 5). Clearly, the E376D mutation is silent as regards to the binding of octenoyl-CoA to the enzyme, but it exhibits just opposite effects on the binding of acetoacetyl-CoA and IACoA ligands to the enzyme, respectively.

Given these results, the question arose whether the above-noted correspondences among the spectral, thermodynamic, and kinetic properties for the binding of individual ligands to the enzyme had some common molecular basis. Based on the UV/visible, CD, and resonance Raman spectroscopy, as well as the X-ray crystallographic data, it is evident that the UV/visible spectral changes upon binding of different CoA-ligands to the enzyme originate due to close proximity of the enzyme-bound FAD and the ligands within the enzyme site phase (*5*, *6*, *8*, *9*, *12*, *18*, *34*). More specifically, the carbonyl oxygen of C_8-CoA is known to be localized (in the X-ray crystallographic structure of the enzyme−C_8-CoA complex) at 2.77 and 2.99 Å distances from the 2′-ribityl oxygen of FAD and the main-chain amide nitrogen of Glu-376, respectively, and thus has a high potential to form strong hydrogen bonds (*7*). Of these, the contribution of hydrogen bonding between the carbonyl oxygen and the main chain amide nitrogen (and its potential to polarize the carbonyl group of the CoA-ligands) is questionable in light of the experimental observation that 2′-deoxy-FAD-substituted enzyme is devoid of catalytic activity (*35*). However, given that the electronic spectrum of the enzyme-bound IACoA is red-shifted, presumably due to an extended conjugation of the π electrons of the indole ring to its carbonyl oxygen (*5*), the hydrogen bonding between the carbonyl oxygen of IACoA and the 2′-ribityl hydroxyl group of FAD is eminent. Resonance Raman spectroscopic studies for the binding of acetoacetyl-CoA to the oxidized form of the enzyme reveal that, besides polarization of the carbonyl oxygen, the α-methylene group of acetoacetyl-CoA acquires an anionic character and forms a charge-transfer complex upon interactions with the C4A and N5 atoms of FAD (*34*). Based on this evidence, we surmise that the distances separating the carbonyl oxygen of the CoA-ligands and the 2′-ribityl hydroxyl of FAD, as well as the α-methylene group of the CoA-ligands and the C4A and N5 atoms of FAD, were

involved in the spectral changes upon binding of different ligands to the enzyme site.

However, it should be emphasized that the observed spectral changes upon binding of all the CoA-ligands (utilized herein) to MCAD do not originate at the instant they bind to the enzyme site (*5, 8, 9, 14, 18, 20*), i.e., upon formation of the enzyme−ligand collision/Michaelis complexes (see eq 3). Instead, such changes originate during the course of a slow isomerization process, which proceeds via an obligatory change in the protein conformation. Hence, the collision and isomerized complexes (see eq 3) have often been referred to as the "colorless" and "colored" complexes, respectively (*5, 13, 27*). In the case of IACoA, it has been explicitly noticed that the overall equilibrium constant of the enzyme−IACoA complex is contributed, to a large extent, by the ratio of the forward (k_2) to the reverse (k_{-2}) rate constants of the isomerization step of eq 3 (*5*). Consequently, any factor that enhanced the forward rate constant (k_2) or diminished the reverse rate constant (k_{-2}) resulted in a decrease in the dissociation constant (i.e., increase in the binding affinity) of the enzyme−IACoA complex (*33*). Aside from these, Qin and Srivastava (*27*) recently provided evidence that the above isomerization step (k_2/k_{-2}) contributes to the overall ΔH° value upon interaction of IACoA with the enzyme. Hence, the changes in the electronic spectrum of IACoA, in the binding affinity of IACoA to the enzyme and its associated thermodynamic parameters, and in the forward and reverse rate constants for the interaction of IACoA with the enzyme are all intrinsic to the slow isomerization step of the enzyme−IACoA collision complex. With precedents of our contemporary studies involving other ligands, a qualitatively similar conclusion can be drawn for the interaction of acetoacetyl-CoA and octenoyl-CoA with the enzyme site (*8, 9, 14, 20*). Therefore, the observed spectral, thermodynamic, and kinetic properties for the binding of ligands to the enzyme appear to have a common molecular origin.

The question arises as to why the Glu-376→Asp mutation in MCAD exhibits a different influence on the spectral, thermodynamic, and kinetic properties for the binding of octenoyl-CoA, acetoacetyl-CoA, and IACoA to the enzyme. A plausible answer to this question comes from the molecular modeling data of the individual enzyme−ligand complexes. As elaborated under Results, the bonding distances between the carbonyl oxygen of the CoA-ligands and the 2′-ribityl OH group of FAD as well as between the α-carbon of the CoA-ligands and the N5 and C4A atoms of FAD are differently affected (involving different CoA-ligands utilized herein) at the active sites of the wild-type and E376D mutant enzymes. However, one may question the reliability of molecular modeling results in providing the structural basis of our observed experimental data. This is particularly true since the maximum difference between the selected atoms of the FAD and CoA-ligands (upon Glu-376→Asp mutation) is less than 1 Å. The above difference may be argued to originate due to artifacts in attaining local energy minima of the enzyme−ligand complexes during the energy minimization protocols. However, there are two arguments against such a possibility. First, the mutation at the enzyme site was introduced following the energy minimizations of the individual wild-type enzyme−ligand complexes. Hence, the corresponding mutant enzyme−ligand complexes had little room to undergo substantial structural changes. This is evident by a small rms deviation between the minimized wild-type and mutant enzyme−ligand complexes. Second, the maximum derivatives of the minimized structures of both wild-type and mutant enzyme−ligand complexes were found to be reasonably low (i.e., in the range of 10^{-4}−10^{-5} kcal mol^{-1} Å^{-1}), which is considered to be ideal for globally minimized structures of enzyme−ligand complexes of comparable dimensions (*30, 31*). In light of these considerations, it appears unlikely that the discriminatory effects of Glu-376→Asp mutation on interatomic distances between selected atoms between the enzyme-bound FAD and CoA-ligands (discerned via the molecular modeling studies) are merely due to a coincidence.

The binding of a ligand to its cognate enzyme site can be envisaged to proceed via three consecutive steps, namely, desolvation, immobilization, and packing (*36*). On kinetic grounds, the first two processes are expected to proceed concomitantly, and on a relatively short time scale. The packing, on the other hand, is likely to be a slower process since it is expected to involve sampling of alternative conformational states of both protein and ligand molecules. In the case of MCAD, the slow isomerization step during the course of binding of different CoA-ligands to the enzyme is likely to be a consequence of packing of the individual atoms of the enzyme and ligands to yield optimally bonded and maximally stable structures of the enzyme−ligand complexes. If an enzyme can accommodate structurally different ligands, the extent of packing would be expected to be different with different ligands. Likewise, if a mutation creates a "void" (e.g., of 1.9 Å radius) at or near the active site of an enzyme (e.g., E376D mutation in the case of MCAD), and such a void is not filled by a water molecule (of 1.4 Å radius), the magnitude of packing of the individual enzyme−ligand complexes would be different with wild-type versus the mutant enzyme. In the case of physiological (naturally selected) ligands, such as octenoyl-CoA, we believe the packing forces at the ω-end of the ligand preclude the mobility near its carbonyl group upon E376D mutation. The above advantage, however, is not realized in the case of acetoacetyl-CoA, presumably due to the shorter carbon tail beyond the thioester group. On the contrary, the bulky indole group of IACoA is preferentially accommodated (by filling the 29 Å^3 created void volume) at the E376D mutant (vis a vis the wild-type) enzyme site. Given these results, we are forced to conclude that the discriminatory influence of Glu-376→Asp mutation on the spectroscopic, thermodynamic, and kinetic properties for the binding of structurally different types of ligands to the enzyme is due to ligand-specific packing (to accommodate the void created by the mutation) of the protein structure.

REFERENCES

1. Beinert, H. (1963) *Enzymes (2nd Ed.) 7*, 447−466.
2. Engel, P. C. (1990) in *Chemistry and Biochemistry of Flavoenzymes* (Muller, F., Ed.) Vol. III, pp 597−655, CRC Press, Inc., London.
3. Thorpe, C., and Kim, J.-J. P. (1995) *FASEB J. 9*, 718−725.
4. Murfin, W. W. (1974) Ph.D. Dissertation, Washington University, St. Louis, MO.
5. Johnson, J. K., Wang, Z. X., and Srivastava, D. K. (1992) *Biochemistry 31*, 10564−10575.

6. Nishina, Y., Sato, K., Hazekawa, I., and Shiga, K. (1995) *J. Biochem. 117*, 800−808.
7. Kim, J.-J. P., Wang, M., and Paschke, R. (1993) *Proc. Natl. Acad. Sci. U.S.A. 90*, 7523−7527.
8. Kumar, N. R., and Srivastava, D. K. (1994) *Biochemistry 33*, 8833−8841.
9. Kumar, N. R., and Srivastava, D. K. (1995) *Biochemistry 34*, 9434−9443.
10. Lehman, T. C., Hale, D. E., Bhala, A., and Thorpe, C. (1990) *Anal. Biochem. 186*, 280−284.
11. Beinert, H. (1963) *Enzymes (2nd Ed.) 7*, 467−476.
12. Kim, J.-J. P., and Wu, J. (1988) *Proc. Natl. Acad. Sci. U.S.A. 85*, 6677−6681.
13. Srivastava, D. K., Kumar, N. R., and Peterson, K. L. (1995) *Biochemistry 34*, 4625−4632.
14. Peterson, K. L., Sergienko, E. E., Wu, Y., Kumar, N. R., Strauss, A. W., Oleson, A. E., Muhonen, W. W., Shabb, J. B., and Srivastava, D. K. (1995) *Biochemistry 34*, 14942−14953.
15. Johnson, J. K., and Srivastava, D. K. (1993) *Biochemistry 32*, 8004−8013.
16. Johnson, J. K., Kumar, N. R., and Srivastava, D. K. (1993) *Biochemistry 32*, 11575−11585.
17. Johnson, J. K., Kumar, N. R., and Srivastava, D. K. (1994) *Biochemistry 33*, 4738−4744.
18. Johnson, J. K. (1994) Ph.D. Dissertation, North Dakota State University, Fargo, ND.
19. Peterson, K. L., and Srivastava, D. K. (1997) *Biochem. J. 325*, 751−760.
20. Kumar, N. R. (1997) Ph.D. Dissertation, North Dakota State University, Fargo, ND.
21. Peterson, K. L., Galitz, D. S., and Srivastava, D. K. (1998) *Biochemistry 37*, 1697−1705.
22. Powell, P. J., and Thorpe, C. (1988) *Biochemistry 27*, 8022−8024.
23. Kumar, N. R., Peterson, K. L., and Srivastava, D. K. (1996) *Flavin and Flavoproteins* (Stevenson, K. J., Massey, V., and Williams, C. W., Eds.) pp 633−636, University of Calgary Press, Calgary.
24. Raines, R. T., Sutton, E. L., Straus, D. R., Gilbert, W., and Knowles, J. R. (1986) *Biochemistry 25*, 7142−7154.
25. Thorpe, C., Matthews, R. G., and Williams, C. W., Jr. (1979) *Biochemistry 18*, 331−337.
26. Bernert, J. T., and Sprecher, H. (1977) *J. Biol. Chem. 252*, 6737−6744.
27. Qin, L., and Srivastava, D. K. (1998) *Biochemistry 37*, 3499−3508.
28. Srivastava, D. K., Wang, S., and Peterson, K. L. (1997) *Biochemistry 36*, 6359−6366.
29. Wiseman, T., Williston, S., Brandt, J. F., and Lin, L.-N. (1989) *Anal. Biochem. 17*, 131−137.
30. Dauber-Osguthorpe, P., Roberts, V. A., Osguthorpe, D. J., Wolff, J., Genest, M., and Hagler, A. T. (1988) *Proteins: Struct., Funct., Genet. 4*, 31−47.
31. Roberts, V. A., Dauber-Osguthorpe, P., Osguthorpe, D. J., Levin, E., and Hagler, A. T. (1986) *Isr. J. Chem. 27*, 327−341.
32. McKean, M. C., Frerman, F. E., and Mielke, D. M. (1979) *J. Biol. Chem. 254*, 2730−2735.
33. Srivastava, D. K., Johnson, J. K., Kumar, N. R., and Peterson, K. L. (1996) *Flavins and Flavoproteins* (Stevensen, K. J., Massey, V., and Williams, C. W., Eds.) pp 641−644, University of Calgary Press, Calgary.
34. Nishina, Y., Sato, K., Shiga, K., Fujii, S., Kuroda, K., and Miura, R. (1992) *J. Biochem. 111*, 699−706.
35. Ghisla, S., Engst, S., Moll, M., Bross, P., Strauss, A. W., and Kim, J.-J. P. (1992) in *New Developments in Fatty Acid Oxidation*, pp 127−142, Wiley-Liss, Inc., New York.
36. Morton, A., Baase, W. A., and Matthews, B. W. (1995) *Biochemistry 34*, 8564−8575.

BI980380P